RESEARCH

CrossMark

Adsorption and inhibitive properties of seroquel drug for the corrosion of zinc in 0.1 M hydrochloric acid solution

A. M. Guruprasad[1] · H. P. Sachin[2] · G. A. Swetha[3] · B. M. Prasanna[4]

Abstract

Inhibition action of seroquel on corrosion of zinc in 0.1 M HCl solution was investigated using weight loss, electrochemical potentiodynamic polarization and impedance spectroscopic techniques. Corrosion inhibition efficiency showed the positive effect with increase in concentration of inhibitor and with the increase in temperature. Results obtained from all the methods are in good agreement with each other. Inhibition effect of inhibitor is due to the adsorption of seroquel molecule on zinc surface from bulk of the solution and the process of adsorption follows Temkin's adsorption isotherm. Potentiodynamic polarization studies revealed that seroquel acts as a mixed type of inhibitor. Corrosion inhibition mechanism is explained by activation and thermodynamic parameters. Surface morphology of the corroded metal was studied by scanning electron microscopic studies and FT-IR spectrum of the corrosion product further confirms the process of adsorption of seroquel on metal surface.

Keywords Zinc · Corrosion inhibition · Acid · Antipsychotic drug · Seroquel · EIS

Introduction

Corrosion is a spontaneous surface phenomenon results in deterioration of metal or alloys when it interacts with surrounding environment. Zinc is one of the most important non-ferrous metals with numerous industrial applications and is mainly used for the corrosion protection of steel [1]. The corrosion of zinc is affected by both alkaline and acid solution and it is more severe in solution having pH lower than 6.0 and higher than 12.5, while within this range the corrosion is very slow [2, 3]. Under destructive condition, Zn metal suffers from corrosion which gives the rust with white color [4]. Industrial processes such as scale removal and cleaning of zinc surfaces with acidic solutions expose zinc to corrosion. Due to this, zinc material becomes unsuitable for industrial applications [5–8]. It has been found that one of the best methods of protecting metals against corrosion involves the use of inhibitors [9, 10]. These are substances that reduce the corrosion of metallic materials by controlling the metal dissolution [11]. Efficiency of an inhibitor is mainly dependent on its ability to get adsorbed on the surface of metal which involves replacement of water molecule at a corroding interface [12].

Inhibitors are organic compounds containing heteroatoms like nitrogen, oxygen, phosphorus and sulfur in its structure [13–22]. Most of the commercial inhibitors are toxic in nature; therefore, replacement by environmentally benign inhibitors is necessary [11]. Presently, there is a trend to replace existing inhibitors such as chromates and cyanides because of their harmful effect to the nature [6].

The majority of the inhibitor used to control the corrosion of zinc was considered to be toxic, and solubility of inhibitor is a major problem in the corrosive medium. So the focus is to use non-toxic medicinal compound to inhibit the corrosion of zinc. Corrosion of Zinc was inhibited using several inhibitor-like guaifenesin [23], ketosulfone [24], floctafenine [25], atenolol [26], N-arylpyrroles [27], anisidines [28], erythromycin [29], and hexamine [2]. The use of

✉ H. P. Sachin
  drhps@jnnce.ac.in

1   Department of Chemistry, Mangalore Institute
    of Technology and Engineering, Moodbidri, Mangalore,
    Karnataka, India

2   Department of Chemistry, Jawaharlal Nehru National College
    of Engineering (JNNCE), Shivamogga, Karnataka, India

3   Department of Chemistry, BMS Institute of Technology,
    Avalahalli, Bangalore, Karnataka, India

4   Department of Chemistry, Jain Institute of Technology,
    Davanagere, Karnataka, India

pharmaceutical compounds offers interesting possibilities for corrosion inhibition due to the presence of heteroatoms like nitrogen, sulfur and oxygen in their structure and is of particular interest because of their safe use, high solubility in water and high molecular size [30].

Several researchers used medicinal compound having the properties like antimalarial, antibacterial, anti-cancer, etc., as corrosion inhibitors for both steel and zinc. Since only a few work was done on the use of antipsychotic drugs as corrosion inhibitor like ziprasidone [31, 32], clozapine [33], etc. Further, our previous report on corrosion inhibition of steel with seroquel has shown good inhibition to corrosion [34], which triggered us to use seroquel to control the corrosion of another industrially important metal like zinc. Further seroquel possess majority of the properties required to be used as corrosion inhibitor, like the presence of electron-rich heteroatoms, i.e., N, S, and O, electron-rich functional groups like –C=N–, –OH, –NH, π electron-rich aromatic ring and good planarity to wrap the surface of metal and easy solubility. So in the present paper, corrosion inhibition of zinc in 0.1 M HCl solution was investigated using seroquel as inhibitor.

Experimental

Material

Zinc metal strips of pure grade 99.6% (Cu 0.17%, Ti 0.075%, Al 0.05%, Pb–Cd 0.003%, Fe 0.002%, Sn 0.001% and Mg 0.0005%, and remainder being Zn) were used to measure the corrosion rate. The metal strips were abraded by silicon carbide emery papers from 220, 480, 800, 1500 and 2000 grade and washed thoroughly with distilled water, degreased with acetone and properly dried. Weight loss studies were carried out in 0.1 M HCl solution using zinc strips with dimensions of $4 \times 2 \times 0.1$ cm^3. Zinc strips with an area of exposure of 1 cm^2 were used for electrochemical studies. The 0.1 M HCl solutions were prepared using AR-grade HCl and double distilled water.

Inhibitor

Seroquel is an antipsychotic drug, used to treat schizophrenia and other bipolar disorder and used as inhibitor for corrosion of zinc in the present study. The IUPAC name of this drug is (2-[2-(4-dibenzo[b,f][1,4]thiazepin-11-yl-1-piperazinyl) ethoxy]-ethanol. Corrosive solution was prepared in 0.1 M HCl, by adding different concentrations of seroquel i.e., from 200 to 1000 ppm. Molecular structure of Seroquel is shown in Fig. 1.
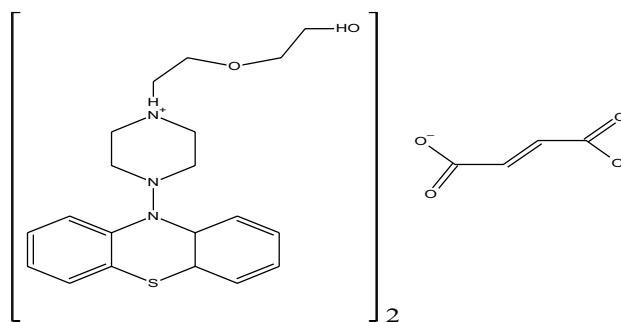

Fig. 1 Molecular structure of seroquel

Weight loss measurements

Weight loss studies were performed by immersing cleaned zinc strips in 100 cm^3 of 0.1 M HCl solution containing different concentration of inhibitor. The experiments were performed at 303–333 K. Experiments were conducted by immersing the metal strips for 6 h in the corrosive medium. The corroded metal strips were taken out, washed with distilled water, dried in acetone and weighed. Measurements were done in triplicate and average values were presented.

Electrochemical measurements

The potentiodynamic polarization and electrochemical impedance spectroscopy (EIS) measurements were carried out using CHI 608D electrochemical analyzer (manufactured by CH Instruments, Austin, USA) at 303–333 K. A three-electrode system with a reference electrode (saturated calomel), working electrode (zinc strip with an area of exposure 1 cm^2) and an auxiliary electrode (platinum) was used for measurements. Prior to each electrochemical measurement, the working electrode was immersed in the solution for 30 min for the open circuit potential to reach a steady state. Polarization curves were recorded at a scan rate of 0.01 V s^{-1} in the potential range of -0.2 to $+0.2$ V to the open circuit potential value (OCP). EIS measurements were performed using the AC signals with amplitude of 5 mV s^{-1} for the frequency spectrum from 10 kHz to 1 Hz. All impedance data were fit to appropriate equivalent circuits (ECs) using the ZSimp Win 3.21 software. The impedance parameters were obtained from Nyquist and Bode's plot.

Scanning electron microscopic studies

Surface morphologies of the metal specimens were recorded using Scanning Electron Microscope (model: VEGA3 TESCAN). For the studies, Zinc specimens were immersed in

0.1 M HCl solution for 6 h in the presence and absence of the seroquel inhibitor. Metal specimens were taken out, washed with distilled water, dried and analyzed by SEM technique. The potential of the accelerating beam employed was 25 kV.

IR spectral studies

FT-IR spectrum of the pure compound and the corrosion product scrapped from the metal surface was carried out using Frontier Perkin Elmer spectrophotometer.

Result and discussions

Weight loss studies

Zinc strips are subjected to weight loss measurements in 0.1 M HCl in the absence and presence of different concentrations of seroquel. The inhibition efficiency (% IE) values and surface coverage (θ) were found to be dependent on the inhibitor concentration. Corrosion inhibition increases steadily with increase in concentrations of inhibitor up to 1000 ppm and were calculated using Eqs. (1) and (2) and tabulated in Table 1. Figure 2 shows the variation of percentage inhibition efficiency with concentration of inhibitor at different temperature:

$$v_{corr} = \frac{\Delta m}{ST} \qquad (1)$$

where Δm is the weight loss difference in the absence and presence of inhibitor, S is the surface area and T is the time of exposure in hours.

The percentage inhibition efficiency is calculated by the following relation:

$$\eta_w(\%) = \frac{v_{corr}^o - v_{corr}}{v_{corr}^o} \times 100 \qquad (2)$$

where v_{corr}^o and v_{corr} are the corrosion rates of zinc in the absence and presence of seroquel, respectively. The results from above observation lead to the conclusion that the compound under investigation is retarding corrosion of zinc in 0.1 M HCl solution. Inhibition efficiency increased with increase in concentration up to 1000 ppm and thereafter the inhibition efficiency remained almost constant. So that the concentration of 1000 ppm is taken as optimum to get higher inhibition. The observed inhibition effects of the seroquel could be attributed to its adsorption on zinc surface. This results in isolation of metal surface from the corrosive medium which reduces the dissolution of the metal by blocking their active corrosion sites.

Polarization studies

Tafel polarization plots were recorded for Zn strips in the absence and presence of various concentration of seroquel molecule at a temperature range of 303–333 K and are shown in Fig. 3. The electrochemical parameters such as corrosion potential (E_{corr}), corrosion current density (i_{corr}), cathodic Tafel slope (β_c), anodic Tafel slope (β_a) and inhibition efficiency (η_p)
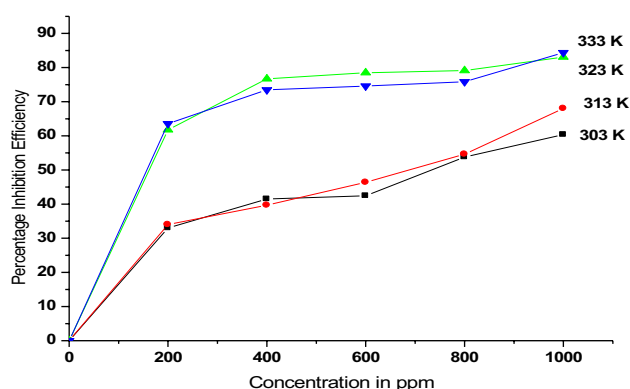

Fig. 2 Variation of corrosion inhibition efficiency in 0.1 M HCl for different concentrations of seroquel at a temperature range of 303–333 K

Table 1 Weight loss results for zinc corrosion inhibition by seroquel in 0.1 M HCl in a temperature range of 303–333 K

Temp	303 K		313 K		323 K		333 K	
C (Concentration in ppm)	(ρ) (g cm^{-2} h^{-1})	η_w (%)	(ρ) (g cm^{-2} h^{-1})	η_w (%)	(ρ) (g cm^{-2} h^{-1})	η_w (%)	(ρ) (g cm^{-2} h^{-1})	η_w (%)
Blank	0.0106	–	0.0194	–	0.1093	–	0.1735	–
200	0.0071	33.01	0.0128	34.02	0.0418	61.75	0.0632	63.57
400	0.0062	41.50	0.0117	39.69	0.0255	76.69	0.046	73.48
600	0.0061	42.45	0.0104	46.39	0.0235	78.49	0.0441	74.58
800	0.0049	53.77	0.0088	54.63	0.228	79.13	0.0419	75.85
1000	0.0042	60.37	0.0062	68.04	0.0185	83.07	0.0271	84.38
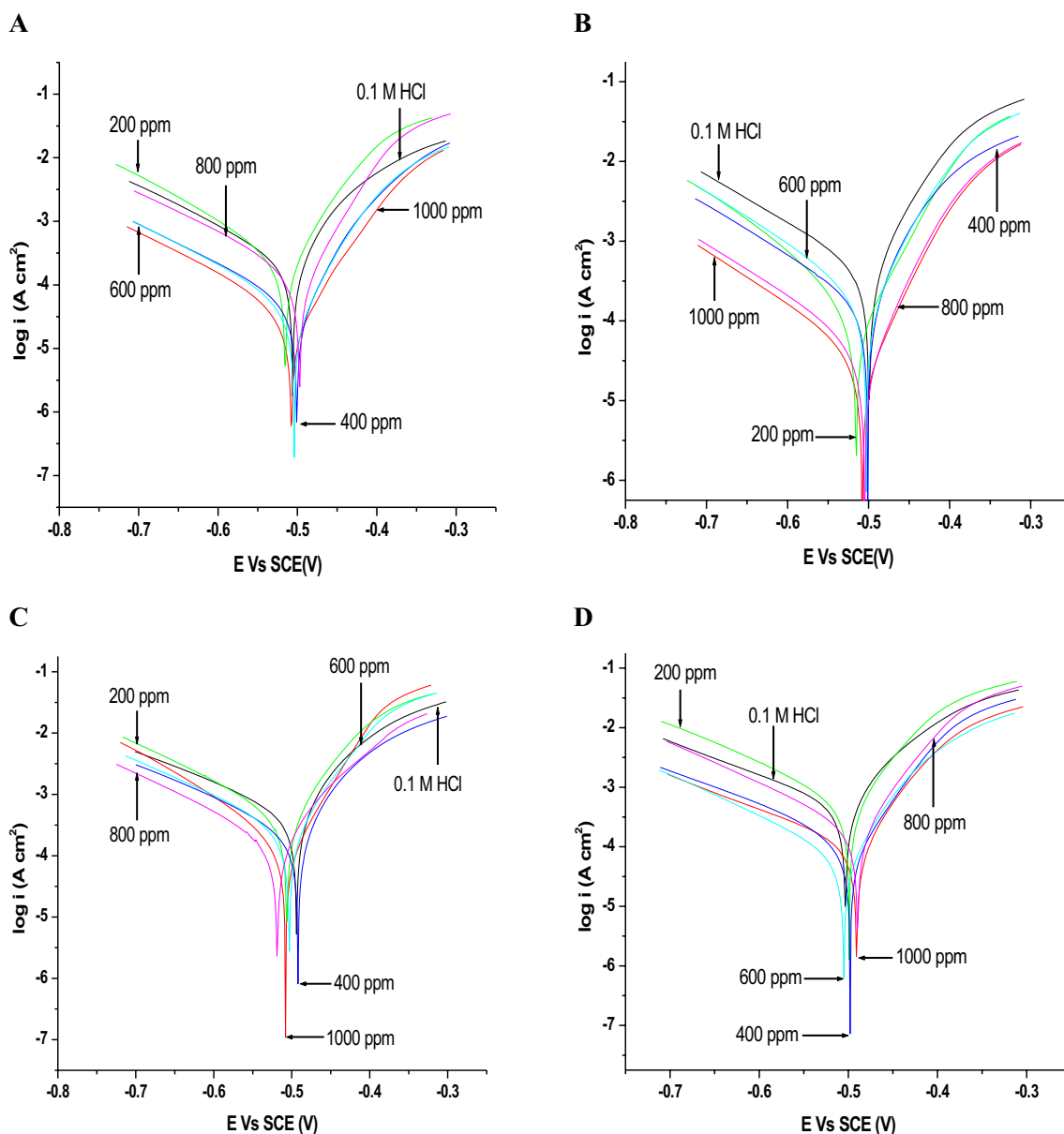
Fig. 3 Tafel plots for zinc specimen in 0.1 M HCl in the absence and presence of different concentrations of inhibitor at **a** 303 K, **b** 313 K, **c** 323 K and **d** 333 K

are given in Table 2. The η_p was calculated from the following relation:

$$\eta_p = \frac{i_{corr}^o - i_{corr}}{i_{corr}^o} \times 100 \tag{3}$$

where i_{corr}^o and i_{corr} are the corrosion current densities in the absence and presence of inhibitor, respectively. From the data available from Table 2, it is clear that corrosion current (i_{corr}) decreases as the inhibitor concentration increases. From Fig. 3, it can be seen that cathodic and anodic polarization curves shifted towards lower current densities in

the presence of inhibitor, indicating effective corrosion mitigation in hydrochloric acid. This can be attributed to decrease in rate of corrosion reaction of the zinc after the addition of inhibitor molecules to the medium. From the data presented in Table 2, it can be seen that the corrosion rate of metal decreased with increase in the concentration of inhibitor molecule at all the studied temperature. This indicates the progressive adsorption of inhibitor on metal surface with increase in concentration. Inhibition efficiency ($\eta_p\%$) of the inhibitor increased with increase in temperature; from this, we can conclude that the seroquel is a better corrosion inhibitor for Zn even at high temperature. After

Table 2 Tafel polarization parameters for zinc corrosion in the absence and presence of seroquel in 0.1 M HCl in a temperature range of 303–333 K

Temp. (K)	Inhibitor conc. (mg L^{-1})	E_{corr} (V)	i_{corr} (A cm^{-2})	Corrosion rate (mpy)	β_c (mV decade^{-1})	β_a (mV decade^{-1})	$\eta_p\%$
	Blank	− 0.506	0.054	18.06	− 7.008	09.648	–
	200	− 0.515	0.039	12.80	− 7.851	14.792	27.77
	400	− 0.501	0.032	09.56	− 6.672	14.608	40.74
303	600	− 0.504	0.025	07.55	− 7.040	16.183	53.70
	800	− 0.507	0.020	05.96	− 6.968	18.302	62.96
	1000	− 0.508	0.016	03.80	− 7.228	17.381	70.37
	Blank	− 0.500	0.094	22.36	− 6.145	13.125	–
	200	− 0.515	0.064	15.30	− 8.661	17.104	31.91
	400	− 0.501	0.040	11.54	− 6.762	11.316	57.44
313	600	− 0.503	0.032	09.51	− 7.329	14.805	65.95
	800	− 0.505	0.024	07.63	− 7.505	17.083	74.46
	1000	− 0.508	0.019	05.76	− 7.154	17.997	79.78
	Blank	− 0.494	0.112	26.64	− 5.842	09.757	–
	200	− 0.506	0.082	19.59	− 6.896	12.602	23.36
	400	− 0.492	0.052	17.44	− 6.320	09.882	53.57
323	600	− 0.503	0.042	12.59	− 6.342	15.501	62.50
	800	− 0.519	0.031	10.18	− 6.859	11.381	72.32
	1000	− 0.508	0.020	07.47	− 7.552	17.837	82.14
	Blank	− 0.503	0.130	31.00	− 5.714	10.620	–
	200	− 0.499	0.107	25.46	− 7.301	12.671	17.69
	400	− 0.498	0.066	20.16	− 6.484	17.166	49.23
333	600	− 0.505	0.052	15.70	− 7.336	13.426	60.00
	800	− 0.490	0.037	12.60	− 7.191	15.897	71.53
	1000	− 0.491	0.023	09.02	− 5.716	14.111	82.30

the addition of inhibitor, the calculated change in corrosion potential (E_{corr}) is not as large as ± 85 mV. It can be interpreted as seroquel is inhibiting both oxidation reaction of zinc at anode and reduction reaction at cathode, i.e., it acts as a mixed type inhibitor [35]. Further, the values of both anodic and cathodic Tafel slopes (β_a and β_c) change by the addition of seroquel to the corrosive medium indicating the influence of inhibitor on both anodic and cathodic reactions, i.e., the added inhibitor adsorbs on the active sites of anode and cathode and controls the corrosion of zinc by controlling metal dissolution as well as hydrogen liberation. So seroquel can be considered to be a mixed type of inhibitor.

## Electrochemical impedance spectroscopy (EIS) measurements

Kinetics of the electrode process and surface properties at the metal–solution interface can be quantitatively explained by Electrochemical Impedance Spectroscopy. EIS is an easy and time-conserving technique for monitoring corrosion process. The results obtained are reliable because the measurements are performed very near to the corrosion potential.

EIS is also a non-destructive test because the magnitude of potential applied is small [36].

Nyquist and Bode's plots were recorded for zinc metal in the absence and presence of different concentration of seroquel in 0.1 M HCl solution at 303–333 K and shown in Figs. 4 and 5, respectively. The measured impedance data were analyzed by fitting into equivalent electrochemical circuit as shown in Fig. 6. The goodness of the fits was in the order of 10^{-4} indicating good correlation with the equivalent circuit model used. The experimental curve was almost exactly fitted with the curve obtained by the electrical equivalent circuit as is shown in Fig. 7. The calculated corrosion parameters like polarization resistance (R_p), double layer capacitance (C_{dl}) and the observed inhibition efficiency ($\eta_z\%$) and the surface coverage value are presented in Table 3.

Nyquist plots shown in Fig. 4 represent that the sizes of the diameters of semicircles are influenced by the presence of seroquel molecule with that of the uninhibited solution, which clearly says the role of seroquel on corrosion rate. The diameter of the semicircle increases as the concentration of seroquel increases up to 1000 ppm, but above that
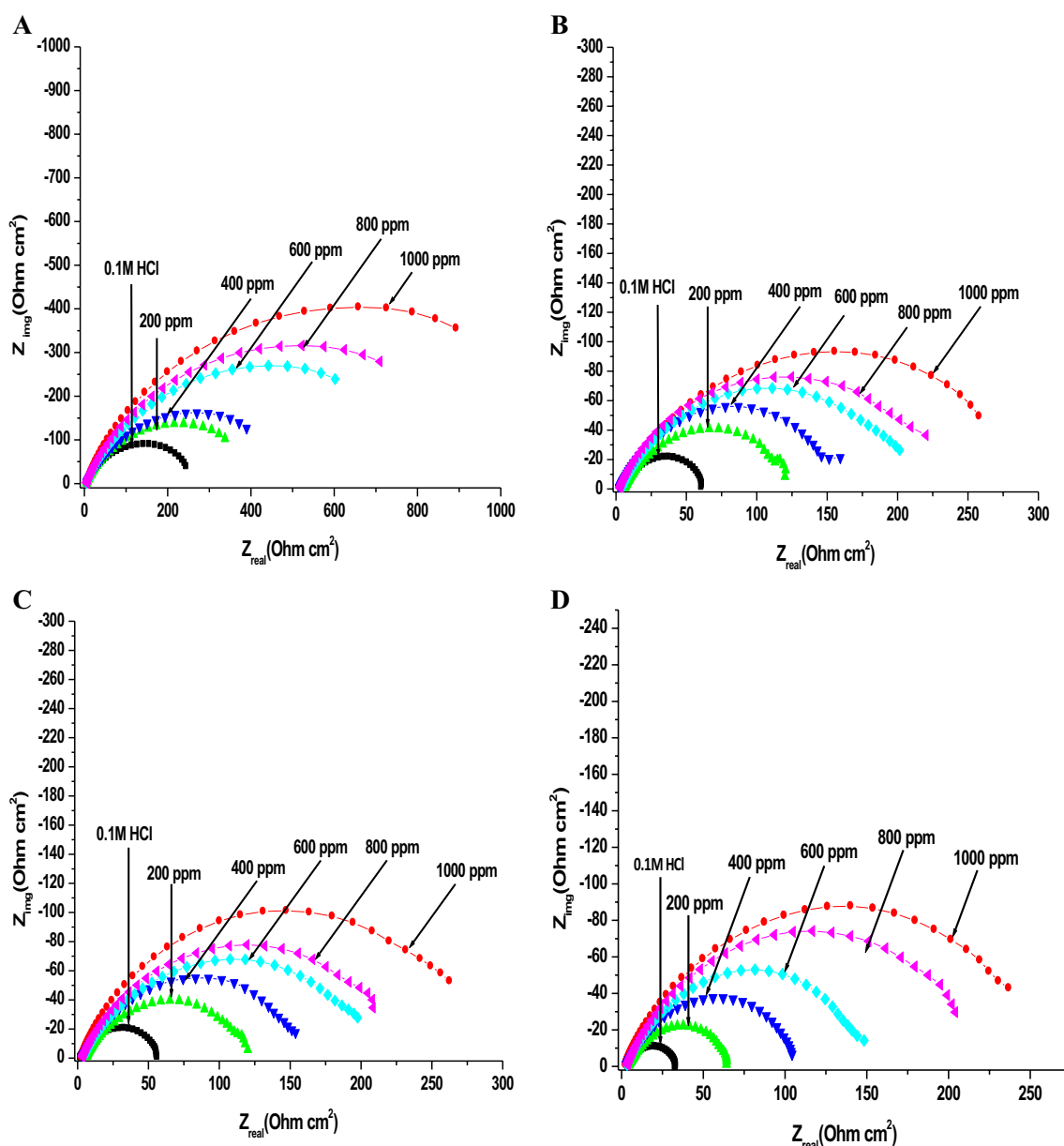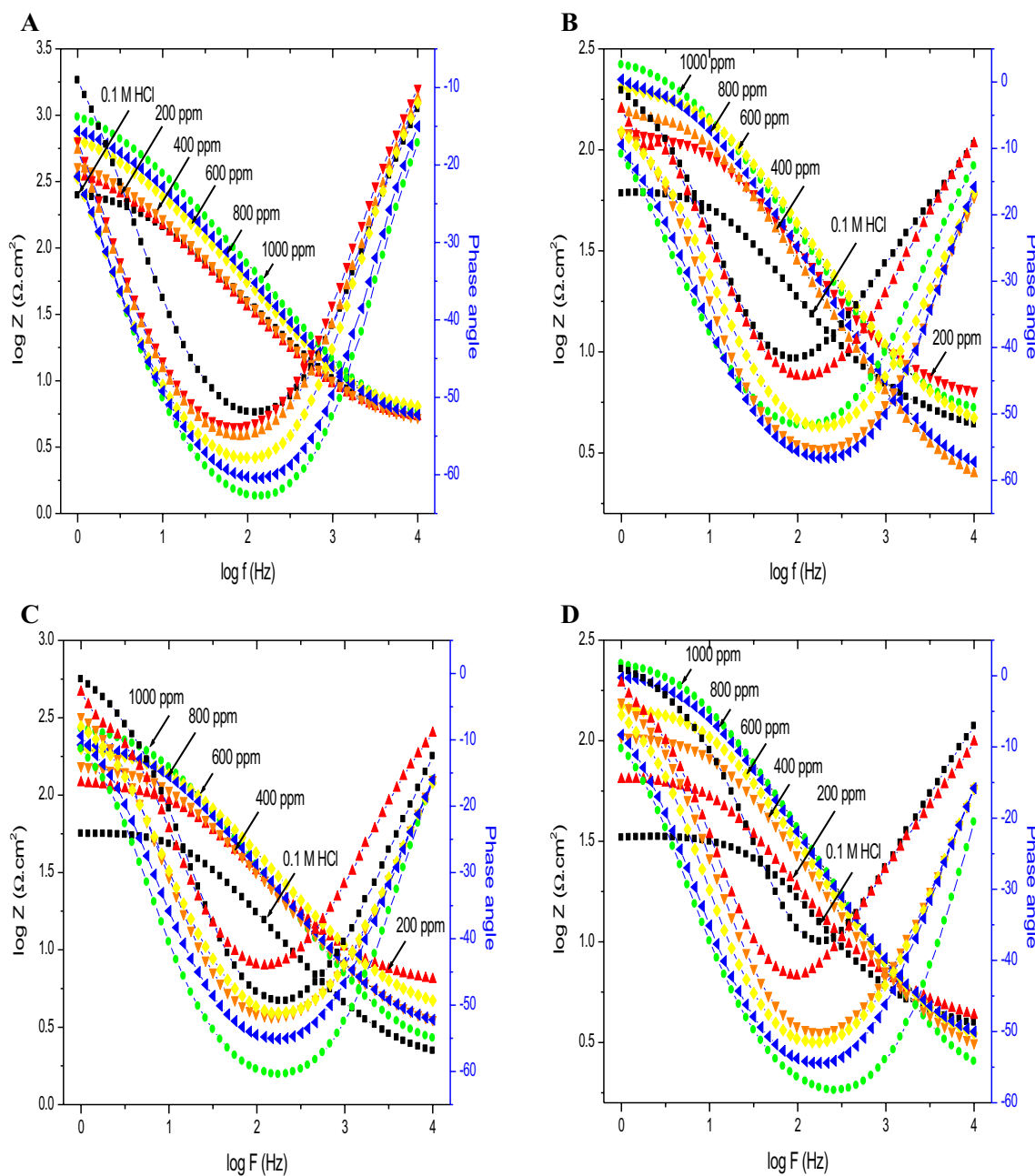
Fig. 4 Nyquist plots for zinc specimen in 0.1 M HCl in the absence and presence of different concentrations of inhibitor at **a** 303 K, **b** 313 K, **c** 323 K and **d** 333 K

no appreciable change was observed. Further, the Nyquist plots produced imperfect single depressed semicircles, which are referred to as frequency dispersion. This is commonly seen in solid electrodes and it is attributed to the roughness and other inhomogeneities of the electrode surface [37, 38].

From the Bodes plot presented in Fig. 5, the depressed semicircle usually obtained for metal–solution interface due to the roughness of the metal surface [36–38]. Corrosion of zinc in acid media results in the increase in roughness of the metal surface, which causes decrease in the phase angle. It was seen from the Bode's plot that phase angle increased

with increase in both inhibitor concentration and temperature. The data further support the progressive adsorption of inhibitor on the metal surface, which blocks the active sites, thereby reducing the corrosion rate.

The values of electrochemical impedance parameters obtained from fitting the experimental data to the used equivalent model are presented in Table 3. The data indicate that, as the inhibitor concentration increases the C_{dl} values decreases, R_p and the inhibition efficiency values increase. Decrease in C_{dl} values with increasing concentration of seroquel is due to increased thickness of electrical double layer suggesting that Seroquel molecule acts by

Fig. 5 Bode plots for zinc specimen in 0.1 M HCl in the absence and presence of different concentrations of inhibitor at **a** 303 K, **b** 313 K, **c** 323 K and **d** 333 K
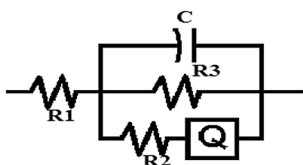
Fig. 6 Electrical equivalent circuit model for impedance data fitting

adsorption at the metal solution interface. Increase in R_p values with concentration of seroquel indicates increase in charge transfer resistance. This assumption is also supported by the increase in the diameter of the capacitive loops with increase in Seroquel concentration.

Impedance study was also carried out at higher temperature from 303 to 333 K and the values are shown in Table 3. It has been found that the value of R_p decreases as the temperature increases in the absence of the inhibitor, which indicates the increase of corrosion at high temperature. But, the
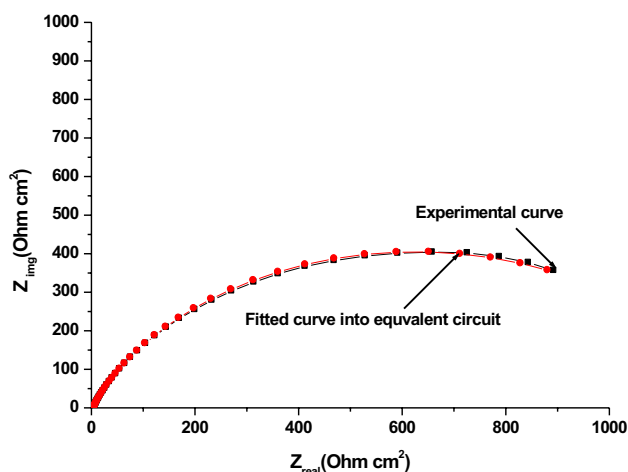
Fig. 7 The experimental curve was fitted with the curve obtained by the electrical equivalent circuit for Nyquist plot in 0.1 M HCl in the presence of 1000 ppm of seroquel

value of R_p increased significantly by the addition of seroquel at high temperature which indicates that the increase of adsorption thereby decreases the corrosion rate.

Sum of charge transfer resistance (R_{ct}) and adsorption resistance (R_{ad}) are equivalent to polarization resistance (R_p) [38]. The percentage inhibition efficiency ($\eta_z\%$) was calculated using the following equation:

$$\eta_z = \frac{R_p - R_p^o}{R_p} \times 100 \tag{4}$$

where R_p and R_p^o are polarization resistance values in the presence and absence of seroquel molecule.

Adsorption isotherm and thermodynamic considerations

It has been found that the organic molecules retard the corrosion of metal by adsorbing on the metal surface. Adsorption of an organic molecule may be referred to be either physical or chemical and it depends on the molecular structure of inhibitor, nature of metal, solution temperature, etc. Vanderwall's force is responsible for physisorption and chemical bonding occur during chemisorption. The ability of seroquel to act as corrosion inhibitor over zinc surface can be interpreted by the use of adsorption isotherms. Langmuir,

Table 3 Electrochemical impedance spectroscopy parameters for zinc corrosion in the absence and presence of seroquel in 0.1 M HCl in a temperature range of 303–333 K

| Temp. (K)	Inhibitor concentration (ppm)	R_p (Ω cm^2)	C_{dl} (F cm^{-2})	Goodness of fit ($\times 10^{-4}$)	$\eta_z\%$	Surface coverage
303	Blank	279.4	0.00219	2.641	–	–
	200	439.6	0.00667	2.998	36.44	0.36
	400	520.2	0.00756	2.432	46.25	0.46
	600	873.6	0.01461	1.589	68.01	0.68
	800	1050	0.01408	1.416	73.39	0.73
	1000	1266	0.01458	0.852	77.93	0.78
313	Blank	62.64	0.01577	5.818	–	–
	200	151.6	0.00859	2.740	58.68	0.59
	400	189.7	0.02208	4.466	66.97	0.67
	600	233.9	0.00352	1.276	73.21	0.73
	800	270.8	0.01139	2.704	76.84	0.77
	1000	298.9	0.01372	1.932	79.04	0.79
323	Blank	39.18	0.01889	5.752	–	–
	200	107.5	0.01227	3.521	63.55	0.64
	400	136.7	0.01543	3.419	71.33	0.71
	600	161.8	0.01119	1.469	75.78	0.76
	800	185	0.01439	1.690	78.82	0.79
	1000	236.8	0.01100	1.823	83.45	0.83
333	Blank	29.68	0.02129	4.172	–	–
	200	57.95	0.02187	4.863	48.78	0.49
	400	120.9	0.01069	3.917	75.45	0.75
	600	169.4	0.01401	3.625	82.47	0.82
	800	182.1	0.01780	2.475	83.70	0.84
	1000	213.9	0.00739	2.115	86.12	0.86

Frumkin, Temkin and Freundlich isotherms were the most considerably utilized isotherms to know the mode of adsorption and to get the information about the nature of interaction between the inhibitor molecules with the metal surface [39]. Surface coverage (θ) for the various concentrations of the tested inhibitor was utilized to elucidate the preferable adsorption isotherm to determine the adsorption process. The adsorption on the corroding surfaces never reaches the real equilibrium and tends to reach an adsorption steady state. When corrosion rate is sufficiently decreased in the presence of inhibitor, the adsorption steady state has a tendency to attain quasi-equilibrium state. Now, it is reasonable to consider quasi-equilibrium adsorption in thermodynamic way using the appropriate adsorption isotherm [38]. Efficiency of an inhibitor increases with increase in adsorbed inhibitor molecules covering the active metal surface. Therefore, surface coverage (θ) can be calculated using Eq. (5):

$$\theta = \% \frac{I \cdot E}{100}.$$ (5)

The stabilization of the adsorbed inhibitor molecules differs according to the type of adsorption that is chemical or physical or both. The surface coverage (θ) values for various concentrations of inhibitor were tested by fitting to various isotherms. The linear regression coefficient (R^2) of Temkin adsorption isotherm in Fig. 8 was found to be closer to unity, hence indicating that the inhibitor under study obeys Temkin adsorption isotherm which may be formulated as:

$$\theta = \frac{1}{f} \ln K_{ads} C$$ (6)

where θ is the degree of surface coverage, C is the inhibitor concentration, K_{ads} denotes the strength between adsorbate and adsorbent and f is the heterogeneous factor of the metal surface describing the molecular interactions in the adsorption layer. If $f > 0$, mutual repulsion of molecules occurs and if $f < 0$ attraction takes place [40].
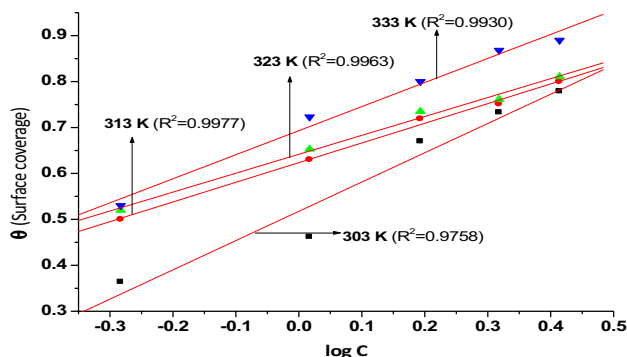
The equilibrium constants K_{ads} are related to the standard adsorption free energy (ΔG^o) as shown in the following equation [41]:

$$K_{ads} = \frac{1}{55.5} e^{\left(\frac{-\Delta G^o_{ads}}{RT}\right)}$$ (7)

where 55.5 (mol L^{-1}) is the molar concentration of water in solution, T (K) is the absolute temperature and R (J mol^{-1} K^{-1}) is the molar gas constant. The K_{ads} and ΔG^o_{ads} values are given in Table 4. The negative values of ΔG^o_{ads} indicate that the adsorption of seroquel on zinc surface is spontaneous. In addition, the higher value of K_{ads} shows that the adsorption of inhibitor is a spontaneous process [24]. Generally, values of ΔG^o_{ads} up to -20 kJ mol^{-1} are consistent with physisorption, while those around -40 kJ mol^{-1} or higher are associated with chemisorption as a result of the sharing or transfer of electrons from organic molecules to the metal surface to form a coordinate bond [42]. The ΔG^o_{ads} values between -29.17 and -31.25 may be indicative of the both physisorption and chemisorption. It is evident from Table 4 that the values of ΔG^o_{ads} decreased with increase in the temperature, which indicates that the adsorption of seroquel is a spontaneous process [43].

A plot of $\Delta G^o_{ads}/T$ versus $1000/T$ is linear (Fig. 9) with the slope equal to ΔH^o_{ads} and intercept to $-\Delta S^o_{ads}$. The change in free energy (ΔG^o_{ads}) of the corrosion process can be calculated at each temperature by applying the equation:

Table 4 Adsorption parameters for inhibition of zinc surface corrosion by seroquel in 0.1 M HCl in a temperature range of 303–333 K

Temperature (K)	K_{ads}	$-\Delta G^o_{ads}$ (kJ mol^{-1})	$-\Delta H^o_{ads}$ (kJ mol^{-1})	$-\Delta S^o_{ads}$ (J mol^{-1} K^{-1})
303	1931.99	29.17	7.82	70.46
313	1603.69	29.65	7.82	69.74
323	1558.28	30.52	7.82	70.27
333	1442.68	31.25	7.82	70.36

Fig. 8 Temkin adsorption isotherm for coverage of seroquel molecules on zinc surface in 0.1 M HCl solution at different temperatures
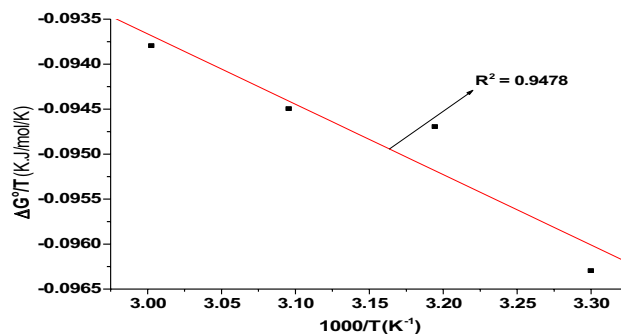
Fig. 9 Relationship between $\Delta G^o_{ads}/T$ and $1000/T$

$$\Delta G_{ads}^{o} = \Delta H_{ads}^{o} - T\Delta S_{ads}^{o}. \tag{8}$$

The enthalpy of adsorption was deduced from the Gibbs–Helmholtz Eq (8):

$$\left\{ \delta \left(\frac{\Delta G_{ads}^{o}/T}{\delta T} \right) \right\}_{p} = -\frac{\Delta H_{ads}^{o}}{T^{2}}. \tag{9}$$

This equation can be rearranged to give the following equation:

$$\Delta S_{ads}^{o} = \frac{(\Delta H_{ads}^{o} - \Delta G_{ads}^{o})}{T}. \tag{10}$$

It is well known that an exothermic adsorption ($\Delta H_{ads}^{o} < 0$) may involve either physisorption or chemisorption or a mixture of both the processes. As the ΔH_{ads}^{o} values obtained are negative, we can say that adsorption of inhibitor on the zinc surface is exothermic process [42]. In this work, ΔS_{ads}^{o} value is found to be negative which indicates that disorder is decreasing with increasing adsorption of seroquel on Zn surface in 0.1 M HCl [44]. Reason for this decrease in entropy may be given as inhibitor molecules were freely moving in the bulk solution (inhibitor molecule were chaotic), but later were adsorbed in an orderly fashion onto the metal surface, resulting in a decrease in entropy. Moreover, from thermodynamic principles, since the adsorption was an exothermic process, it must be accompanied by a decrease in entropy [42, 45].

Activation parameters

The effect of increasing temperature on the corrosion inhibition efficiency of seroquel on zinc in 0.1 M HCl solution was studied at a temperature range (303–333 K) in the absence and presence of different concentrations of inhibitor molecule. This can be known using Arrhenius equation and transition state equation, which can be given as:

$$\ln v_{corr} = \ln A - \frac{E_{a}}{RT} \tag{11}$$

$$v_{corr} = \frac{RT}{Nh} e^{\frac{\Delta S^{*}}{R}} e^{\frac{\Delta H^{*}}{RT}} \tag{12}$$

where v_{corr} is the corrosion rate, A is the frequency factor, h is the Planck's constant, N is Avogadro's number, R is the molar gas constant, T is the absolute temperature, E_{a} is the apparent activation energy, ΔH^{*} is the enthalpy of activation and ΔS^{*} is the entropy of activation.

Figure 10 represents Arrhenius plot which gives a relation between ($\ln v_{corr}$) v/s 1000/T in the form of straight lines for the corrosion of zinc in 0.1 M HCl solution in the absence
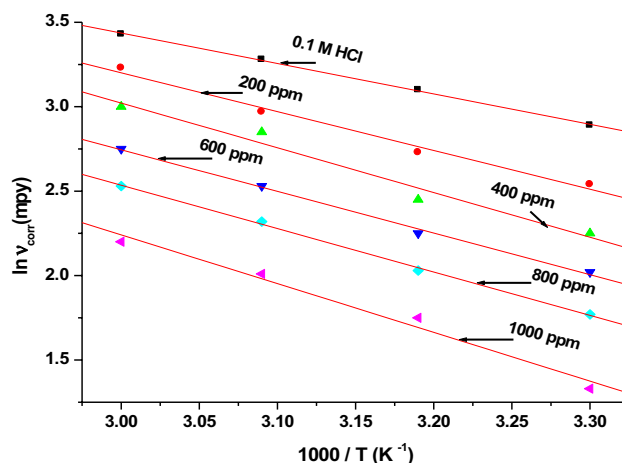

Fig. 10 Arrhenius plot for zinc corrosion in 0.1 M HCl in the absence and presence of different concentrations of seroquel

and presence of inhibitor molecules at different concentrations. From Fig. 10, we can get information about Arrhenius factor A and the apparent activation energy E_{a}. The apparent activation energy corresponding to different concentration was calculated using the formula $E_{a} = (\text{slope} \times R)$ and along with Arrhenius factor A and it is tabulated in Table 5. The increase in E_{a} values in the presence of inhibitor when compared to blank solution indicates the strong adsorption of inhibitor molecules on the zinc surface [46, 47]. This may be explained as with increased adsorption of inhibitor molecules on the zinc surface creates an energy barrier for the spontaneous corrosion reaction on the zinc surface.

Figure 11 represents Transition plot which gives a relation between $\ln(v_{corr}/T)$ v/s 1000/T in the form of straight lines for the corrosion of zinc in 0.1 M HCl solution in the absence and presence of inhibitor molecules at different concentrations. The enthalpy of activation and the entropy of activation were calculated by the formula $\Delta H^{*} = -\text{slope} \times R$, $\Delta S^{*} = \text{intercept} - \ln(R/Nh)$, respectively. For different concentrations, both ΔH^{*} and ΔS^{*} are calculated and tabulated in Table 5. The increase in positive sign of ΔH^{*} indicates that the endothermic nature of the process, suggesting that the dissolution of zinc is slow, may be due to the formation of an energy barrier [48]. The $-\Delta S^{*}$ values were found to be increasing which can be interpreted, as the activated complex in the rate-determining step represents a dissociation rather than an association, meaning that a decrease in disordering takes place going from reactants to the activated complex [49–51]. This is may be due to the orderly adsorption of inhibitor molecules on the zinc surface.

From the above observation, we can conclude that at low temperature, physisorption favors, whereas with increase in temperature, it follows chemical adsorption resulting in the formation of chemical bonding, which makes the molecule

Table 5 Activation parameters for inhibition of zinc surface corrosion by seroquel in 0.1 M HCl in a temperature range of 303–333 K

Concentration (C) (ppm)	E_a (kJ mol^{-1})	A (g cm^{-2} h^{-1})	ΔH^* (kJ mol^{-1})	ΔS^* (J mol^{-1} K^{-1})
Blank	14.96	6.9×10^8	12.42	-21.73
200	19.03	1.2×10^{10}	16.36	-20.55
400	21.94	9.3×10^{10}	19.44	-19.61
600	20.50	1.3×10^{10}	18.01	-20.41
800	21.35	1.7×10^{10}	18.86	-20.40
1000	24.00	7.9×10^{10}	21.25	-19.74
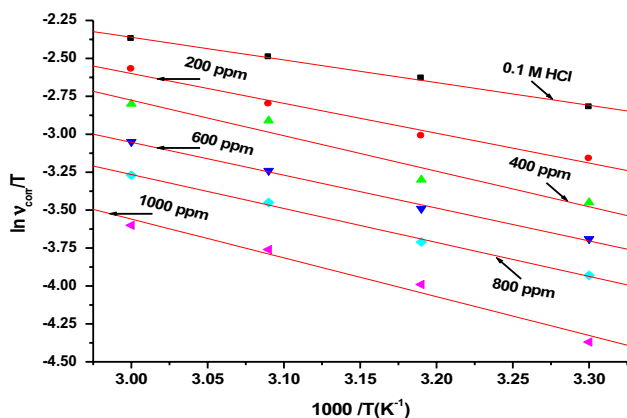
Fig. 11 Transition plot for zinc corrosion in 0.1 M HCl in the absence and presence of different concentrations of seroquel

form a strong barrier between the metal surface and corroding medium which results in increase in inhibition efficiency with increasing temperature.

Scanning electron microscopy (SEM)

The surface morphology of zinc surface in 0.1 M HCl was recorded using scanning electron microscope. The SEM can investigate the changes in the morphological characteristics of the metal surface in the absence and presence of inhibitor [52, 53]. SEM images for zinc immersed in 0.1 M HCl for 6 h duration in the absence and in the presence of optimized concentrations of seroquel are shown in Fig. 12a, b, respectively. A great degree of corrosion can be seen on the zinc surface which was exposed to corrodent (acid) but the zinc surface was remarkably protected by 1000 ppm of seroquel, when it is added to the corrodent. This indicates that seroquel may have formed a protective film around zinc surface resulting in decrease in rate of destruction of the metal surface by the corrosion reaction.
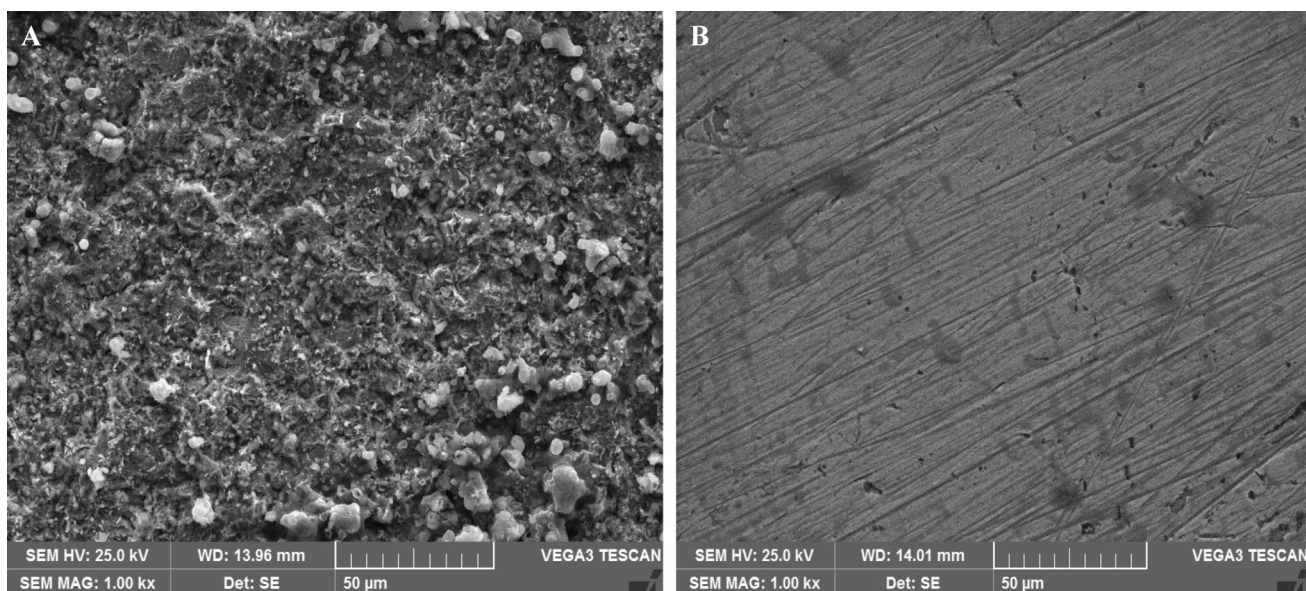
Fig. 12 SEM micrograph of zinc sample surface immersed in 0.1 M HCl at 303 K (**a**) in the absence of seroquel inhibitor (**b**) in the presence of 1000 ppm of seroquel inhibitor
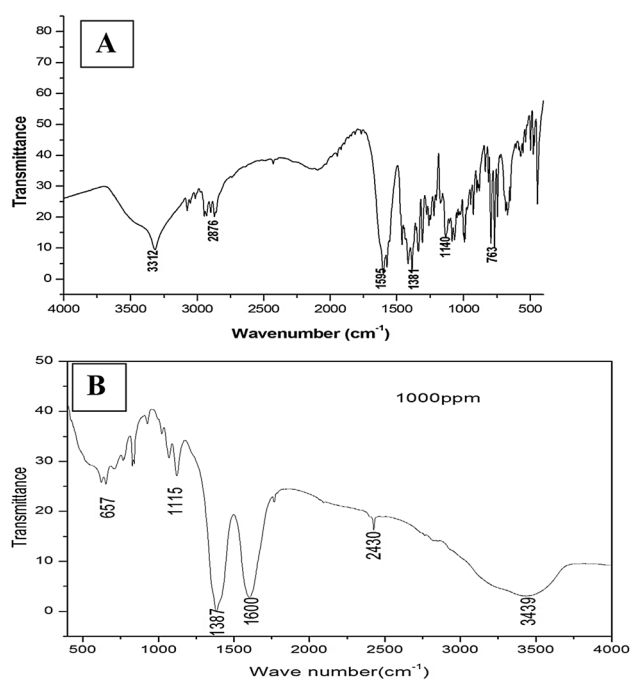
Fig. 13 **a** FT-IR spectrum of seroquel drug; **b** FT-IR spectrum of compound scrapped from corroded metal surface

FT-IR spectral analysis

The structure of the seroquel drug was confirmed by FT-IR spectrum and is shown in Fig. 13a. The presence of broad band at 3312 cm^{-1} indicates the presence of hydroxyl group stretching vibration. The peak at 2876 cm^{-1} is attributed to the presence of carboxylic acid O–H stretching vibration. The peak at 1595 cm^{-1} shows the presence of aromatic C=C bending vibration. The narrow peak at 1381 cm^{-1} is due to C–H absorption. The presence of narrow band at 1140 cm^{-1} is due to the C–O group. The peak at 763 cm^{-1} shows the presence of aromatic C–H bending vibration.

FT-IR analysis was also carried out to understand the interaction between the zinc surface and the inhibitor molecules. Figure 13b shows the FT-IR spectrum of scratched compound from zinc surface after corrosion. The presence of broad absorption peak at 3439 cm^{-1} attributed to the presence of hydroxyl group stretching vibration. The small peak at 2430 cm^{-1} ascribed to O–H stretch from the strong hydrogen bond with –COOH. The peak at 1600 cm^{-1} shows the presence of alkene C=C bending vibration. The narrow peak at 1387 cm^{-1} is due to –CH$_3$ bending mode. The presence of narrow band at 1115 cm^{-1} is due to the C–O group. The peak at 657 cm^{-1} shows the presence of alkyne C–H bending vibration. The slight shift in absorption frequency [54] confirms the interaction of seroquel with metal surface.

Mechanism of inhibition

The information obtained from the IR spectrum of pure seroquel molecule and the corrosion product scrapped from the metal surface clearly indicates the involvement of seroquel in the corrosion inhibition. Generally, corrosion inhibitors adsorb on the metal surface from aqueous solution, thereby blocking the active sites of metal which are susceptible to corrosion. Adsorption of organic molecule happens through the electroactive functional groups, by donor–acceptor interaction with the vacant orbital of metal through coordinate bond. Since seroquel contains more number of electron-rich functional groups, like N, S, O and π electron-rich aromatic ring, it coordinates with metal through these heteroatoms and functional groups and results in reduction in the corrosion rate. In Fig. 13b, appearance of peak at 3439 cm^{-1} compared to 3312 cm^{-1} of pure compound (Fig. 13a) indicates the coordination of seroquel through –OH group. The appearance of peak at 2430 cm^{-1} compared to 2876 cm^{-1} shows the coordination through –OH group of carboxylic acid functional group. Slight shift in the wave number of the absorption peaks and appearance of peak corresponding to the different functional group of seroquel molecule in the IR spectrum of scrapped compound confirm the interaction of the seroquel with zinc metal and result in corrosion inhibition.

Conclusions

The corrosion of zinc in 0.1 M HCl was effectively reduced by seroquel drug molecule. The efficiency of corrosion inhibitor increases with increase in concentration and with increase in temperature. The inhibition efficiency of seroquel on zinc surface from the weight loss method is 84.38% at 333 K, which is in good agreement with inhibition efficiency of Tafel polarization (82.30%) and EIS (86.12%) at 333 K. From polarization curves, we can say that inhibitor acts as a mixed type inhibitor, which means that it reduces both anodic and cathodic corrosion reaction on the zinc surface. Adsorption of seroquel on the zinc surface followed Temkin adsorption isotherm by considering the experimental data obtained for different concentrations of inhibitor at different temperature. The values of ΔG^o_{ads} are found to be negative and less than 40 kJ mol^{-1}. The values of E_a increased in the presence of inhibitor when compared to blank. By these results, we can say that adsorption process is spontaneous. The corrosion product of zinc metal in the presence of seroquel is IR active and not IR active in the absence of inhibitor. From this, we can say that the adsorption of seroquel drug on the zinc surface has decreased the rate of corrosion. Furthermore, this is confirmed by SEM analysis.

After detailed analysis of all the aspects, it can be said that seroquel is an excellent environmentally benign corrosion inhibitor for zinc.

References

1. Khulood S, Khalil KS (2014) Corrosion inhibition of zinc in hydrochloric acid solution using ampicillin. Iraqi J Sci 55:295–303
2. Vashi RT, Desai K (2012) Hexamine as corrosion inhibitor for zinc in hydrochloric acid. Der Pharma Chem 4(5):2117–2123
3. Chaudhari HG, Mahida MM (2012) Aliphatic amines as corrosion inhibitors for zinc in hydrochloric acid. Der Pharm Chem 4:2305
4. Shanbhag A, Venkatesha TV, Prabhu R, Praveen B (2011) Inhibition effects of acetyl coumarines and thiazole derivatives on corrosion of zinc in acidic medium. Bull Mater Sci 34(3):571
5. Shah MD, Patel AS, Mudaliar GV, Shah NK (2011) Schiff bases of triethylenetetramine as corrosion inhibitors of zinc in hydrochloric acid. Chem Port Electrochem Acta 29:101
6. Hebbar N, Praveen BM, Prasanna BM, Venkatesha TV (2015) Inhibition effect of an anti-HIV drug on the corrosion of zinc in acidic medium. Trans Indian Inst Met 68(4):543–551
7. Solomon MM, Umoren SA, Udosoro II, Udoh AP (2010) Inhibitive and adsorptive behaviour of carboxy methyl cellulose on mild steel corrosion in sulphuric acid solution. Corros Sci 52:1317–1325
8. Ade SB, Shitole NV, Lonkar SM (2014) Antifungal drug's used as metal corrosion inhibitor in various acid medium. Int J ChemTech Res 6(7):3642–3650
9. Karthik G, Sundaravadivelu M (2016) Studies on the inhibition of mild steel corrosion in hydrochloric acid solution by atenolol drug. Egypt J Pet 25:183–191
10. Karthikeyan S (2016) Drugs/antibiotics as potential corrosion inhibitors for metals—a review. Int J Chem Tech Res 9(6):251–259
11. Abdel Hameed RS, AlShafey HI, Abu-Nawwas AH (2014) 2-(2, 6-dichloranilino) phenyl acetic acid drugs as eco-Friendly corrosion inhibitors for mild steel in 1 M HCl. Int J Electrochem Sci 9:6006–6019
12. Fouda AS, El-Haddad MN, Abdallah YM (2013) Septazole: antibacterial drug as a green corrosion inhibitor for copper in hydrochloric acid solutions. IJIRSET 2(12):7073
13. Ansari KR, Quraishi MA, Singh A (2017) Chromenopyridin derivatives as environmentally benign corrosion inhibitors for N80 steel in 15% HCl. J Assoc Arab Univ Basic Appl Sci 22:45–54
14. Aribo S, Olusegun SJ, Ibhadiyi LJ, Oyetunji A, Folorunso DO (2017) Green inhibitors for corrosion protection in acidizing oilfield environment. J Assoc Arab Univ Basic Appl Sci 24:34–38
15. Geethamani P, Kasthuri PK (2015) Adsorption and corrosion inhibition of mild steel in acidic media by expired pharmaceutical drug. Cogent Chem 1(1):1091558
16. Paul L, Machunda RL (2016) Investigation of aloe lateritia gel as corrosion inhibitor for mild steel in 2 M HNO_3 and 1 M H_2SO_4 media. J Miner Mater Charact Eng 4:33–39
17. Nazeer AA, El-Abbasy HM, Fouda AS (2013) Antibacterial drugs as environmentally-friendly corrosion inhibitors for carbon steel in acid medium. Res Chem Intermed 39:921–939
18. Al-Amiery AA, Kassim FAB, Kadhuml AAH, Mohamad AB (2016) Synthesis and characterization of a novel eco-friendly corrosion inhibition for mild steel in 1 M hydrochloric acid. Sci Rep 6:19890
19. Zaafarany IA (2013) Corrosion inhibition of mild steel in hydrochloric acid solution using cationic surfactant olyel-amido derivatives. Int J Electrochem Sci 8:9531–9542
20. Abdallah M, Hazazi OA, Al Jahdaly BA, Fouda AS, El-Nagar W (2014) Corrosion inhibition of zinc in sodium hydroxide solutions using coumarin derivatives. IJIRSET 3(6):13802–13819
21. Fouda AS, Mahmoud WM, Abdul Mageed HA (2016) Evaluation of an expired non-toxic amlodipine besylate drug as a corrosion inhibitor for low-carbon steel in hydrochloric acid solutions. J Bio Tribo Corros 2(7):1
22. Guruprasad AM, Sachin HP, Swetha GA (2018) Study of corrosion inhibition of mild steel by capacitabine in hydrochloric acid media. Asian J Chem 30(7):1629–1633
23. Adil H (2015) Corrosion inhibition of zinc metal in 2 M hydrochloric acid solution by using guaifenesin drug as an inhibitor and theoretical calculations. J AlNahrain Univ 18(1):60–65
24. Hebbar N, Praveen BM, Prasanna BM, Venkatesha TV (2015) Corrosion inhibition behaviour of ketosulfone for zinc in acidic medium. J Fundam Appl Sci 7(2):271–289
25. Hebbar N, Praveen BM, Prasanna BM, Venkatesha TV (2015) Anticorrosion potential of a pharmaceutical intermediate floctafenine for zinc in 0.1 M HCl solution. Int J Ind Chem 6(3):221–231
26. Atheel HA, Dhuha HF, Ali AA, Abdul Hameed F, Yousif E (2017) Inhibitive effect of atenolol on the corrosion of zinc in hydrochloric acid. Rasayan J Chem 10(3):922–928
27. Stupnisek-Lisac E, Podbrscek S, Soric T (1994) Non-toxic organic zinc corrosion inhibitors in hydrochloric acid. J Appl Electrochem 24:779–784
28. Vashi RT, Naik D (2010) Anisidines as corrosion inhibitors for zinc in phosphoric acid. Asian J Chem 22(10):7761–7770
29. Eddy NO, Odoemelam SA, Ogoko EC, Ita BI (2010) Inhibition of the corrosion of zinc in 0.01–0.04 M H_2SO_4 by erythromycin. Port Electrochim Acta 28(1):15–26
30. Gece G (2011) Drugs: a review of promising novel corrosion inhibitors. Corros Sci 53:3873–3898
31. Shylesha BS, Venkatesha TV, Praveen BM (2011) Ziprasidone as a corrosion inhibitor for zinc in different acid medium. J Chem Pharm Res 3(1):501–507
32. Nataraja SE, Venkatesha TV, Tandon HC, Shylesha BS (2011) Quantum chemical and experimental characterization of the effect of ziprasidone on the corrosion inhibition of steel in acid media. Corros Sci 53:4109–4117
33. Lgaz H, Salghi R, Jodeh S, Hammouti B (2017) Effect of clozapine on inhibition of mild steel corrosion in 1.0 M HCl medium. J Mol Liq 225:271–280
34. Swetha GA, Sachin HP, Guruprasad AM, Prasanna BM, Sudheer Kumar KH (2018) Use of seroquel as an effective corrosion inhibitor for low carbon steel in 1 M HCl. J Bio Tribo Corros 4:57
35. Hebbar N, Praveen BM, Prasanna BM, Sachin HP (2018) Anticorrosion potential of flectofenine on mild steel in hydrochloric acid media: experimental and theoretical study. J Fail Anal Prev 1(11):371
36. Prasanna BM, Praveen BM, Hebbar N, Venkatesha TV, Tandon HC (2015) Inhibition study of mild steel corrosion in 1 M hydrochloric acid solution by 2-chloro 3-formyl quinoline. Int J Ind Chem. https://doi.org/10.1007/s40090-015-0064-6

37. Ituen EB, Akaranta O, James AO, Shuangqin S (2016) Green anti-corrosive oilfield chemicals from seed and leave extracts of *Griffonia simplicifolia* for mild steel. J Chem Mater Res 5(3):45–57

38. Singh AK, Ebenso EE (2012) Effect of ceftezole on the corrosion of mild steel in HCl solution. Int J Electrochem Sci 7:2349–2360

39. Al-Azawi KF, Al-Baghdadi SB, Mohamed AZ, Al-Amiery AA, Abed TK, Mohammed SA, Kadhum AAH, Mohamad AB (2016) Synthesis, inhibition effects and quantum chemical studies of a novel coumarin derivative on the corrosion of mild steel in a hydrochloric acid solution. Chem Cent J 10(23):1

40. Fouda AS, Abd El-Maksoud SA, Mostafa HM (2017) Tilia leafs as eco-friendly corrosion inhibitor for mild steel in aqueous solutions. Zastita Materijala 58(3):271–282

41. Zhao Q, Tang T, Dang P, Zhang Z, Wang F (2017) The corrosion inhibition effect of triazinedithiol inhibitors for aluminium alloy in a 1 M HCl solution. Metals 7(2):44

42. Ebenso EE, Obot IB (2010) Inhibitive properties, thermodynamic characterization and quantum chemical studies of secnidazole on mild steel corrosion in acidic medium. Int J Electrochem Sci 5:2012–2035

43. Douadi T, Hamani H, Daoud D, Al-Noaimi M, Chafaa S (2016) Effect of temperature and hydrodynamic conditions on corrosion inhibition of an azomethine compounds for mild steel in 1 M HCl solution. J Taiwan Inst Chem Eng 71:388

44. Fouda AS, Rashwan S, Emam A, El-Morsy FE (2018) Corrosion inhibition of zinc in acid medium using some novel organic compounds. Int J Electrochem Sci 13:3719–3744

45. Abdel Hameed RS, Ismail EA, Abu-Nawwas AH, Al-Shafey HI (2015) Expired voltaren drugs as corrosion inhibitor for aluminium in hydrochloric acid. Int J Electrochem Sci 10:2098–2109

46. Abdallah M, Zaafarany IA, Al Jahdaly BA (2016) Corrosion inhibition of zinc in hydrochloric acid using some antibiotic drugs. J Mater Environ Sci 7(4):1107–1118

47. Kolo AM, Idris S, Bamishaiye OM (2018) Corrosion inhibition potential of ethanol extract of *Bryophyllum pinnatum* leaves for zinc in acidic medium. Edelweiss Appl Sci Technol 1(2):17–24

48. Obi-Egbedi NO, Essien KE, Obot IB (2011) Computational simulation and corrosion inhibitive potential of alloxazine for mild steel in 1 M HCl. J Comput Method Mol Des 1(1):26–43

49. Prasanna BM, Praveen BM, Narayana Hebbar BM, Venkatesha TV, Tandon HC (2014) Ketosulfone drug as a green corrosion inhibitor for mild steel in acidic medium. Ind Eng Chem Res 53:8436–8444

50. Karthikaiselvi R, Subhashini S (2014) Study of adsorption properties and inhibition of mild steel corrosion in hydrochloric acid media by water soluble composite poly (vinyl alcohol-omethoxy aniline). J Assoc Arab Univ Basic Appl Sci 16:74–82

51. Ramesh Saliyan V, Vasudeva Adhikari A (2008) Inhibition of corrosion of mild steel in acid media by N′-benzylidene-3-(quinolin-4-ylthio)propanohydrazide. Bull Mater Sci 31(4):699–711

52. Shokri A, Rabiee F, Mahanpoor K (2017) Employing a novel nanocatalyst (Mn/Iranian hematite) for oxidation of SO_2 pollutant in aqueous environment. Int J Environ Sci Technol 14:2485–2494

53. Shokri A, Mahanpoor K, Soodbar D (2016) Degradation of 2-nitrophenol from petrochemical waste water by $UV/NiFe_2O_4/$ Clinoptilolite process. Fresenius Environ Bull 25(2):500–508

54. Shokri A, Mahanpoor K, Soodbar D (2015) Evaluation of a modified TiO_2 ($GO-B-TiO_2$) photo catalyst for degradation of 4-nitrophenol in petrochemical wastewater by response surface methodology based on the central composite design. J Environ Chem Eng 4(1):585–598